

IRE1B degrades RNAs encoding proteins that interfere with the induction of autophagy by ER stress in *Arabidopsis thaliana*

Yan Bao, Yunting Pu, Xiang Yu, Brian D. Gregory, Renu Srivastava, Stephen H. Howell & Diane C. Bassham

To cite this article: Yan Bao, Yunting Pu, Xiang Yu, Brian D. Gregory, Renu Srivastava, Stephen H. Howell & Diane C. Bassham (2018): IRE1B degrades RNAs encoding proteins that interfere with the induction of autophagy by ER stress in *Arabidopsis thaliana*, *Autophagy*, DOI: [10.1080/15548627.2018.1462426](https://doi.org/10.1080/15548627.2018.1462426)

To link to this article: <https://doi.org/10.1080/15548627.2018.1462426>



Accepted author version posted online: 25 Jun 2018.



Submit your article to this journal [↗](#)



Article views: 59



View Crossmark data [↗](#)

Publisher: Taylor & Francis & Taylor and Francis Group, LLC

Journal: *Autophagy*

DOI: 10.1080/15548627.2018.1462426

**IRE1B degrades RNAs encoding proteins that interfere with the induction of
autophagy by ER stress in *Arabidopsis thaliana***

Yan Bao^a, Yunting Pu^{a,b}, Xiang Yu^c, Brian D. Gregory^c, Renu Srivastava^d, Stephen H. Howell^{a,d},
Diane C. Bassham^{a,b,1}

^a Department of Genetics, Development and Cell Biology, Iowa State University, Ames, IA
50011, USA

^b Interdepartmental Genetics and Genomics Program, Iowa State University, Ames, IA 50011,
USA

^c Department of Biology, University of Pennsylvania, Philadelphia, Pennsylvania 19104, USA

^d Plant Sciences Institute, Iowa State University, Ames, IA 50011, USA

¹ Address correspondence to Diane Bassham, bassham@iastate.edu, tel +515-294-7461

Email addresses: Yan Bao, baoyan@msu.edu; Yunting Pu, ypu@iastate.edu; Xiang Yu,
yuxiang8605@gmail.com; Brian Gregory, bdgregor@sas.upenn.edu; Renu Srivastava,
renu@iastate.edu; Stephen Howell, shh@iastate.edu.

Keywords: *Arabidopsis*; autophagosome; autophagy; ER stress; IRE1; mRNA degradation;
RIDD

Abbreviations: ACT2, actin 2; ATG, autophagy-related; BGLU21, β -glucosidase 21; BIP3, binding protein 3; BZIP, basic leucine zipper; DAPI, 4', 6-diamidino-2-phenylindole; DTT, dithiothreitol; ER, endoplasmic reticulum; ERN1, endoplasmic reticulum to nucleus signaling 1; IRE1, inositol requiring 1; GFP, green fluorescence protein; MAP3K5/ASK1, mitogen-activated protein kinase kinase kinase 5; MAPK8/JNK1, mitogen-activated protein kinase 8/c-Jun N-terminal kinase 1; MDC, monodansylcadaverine; PR-14, pathogenesis-related protein 14; RIDD, Regulated IRE1-Dependent Decay of Messenger RNA; ROSY1/ML, interactor of synaptotagmin1/MD2-related lipid recognition protein; Tm, tunicamycin; UPR, unfolded protein response; WT, wild-type.

Conflict-of-interest and financial disclosure: none

Running Title: RIDD regulates plant ER stress-induced autophagy

A. Please enhance the abbreviation list with other genes, gene products, major compounds and terms that are mentioned a minimum of three times in the manuscript.

B. Please carefully review and update whenever pertinent, the nomenclature, acronyms and fonts in the figures, as well as the main and supplementary tables, according to the edited text.

Abstract

Macroautophagy/autophagy is a conserved process in eukaryotes that contributes to cell survival in response to stress. Previously, we found that endoplasmic reticulum (ER) stress induces autophagy in plants via a pathway dependent upon AT5G24360/IRE1B (INOSITOL REQUIRING 1-1), an ER membrane-anchored factor involved in the splicing of AT1G42990/BZIP60 (basic leucine zipper protein 60) mRNA. IRE1B is a dual protein kinase and ribonuclease, and here we determined the involvement of the protein kinase catalytic domain, nucleotide binding and RNase domains of IRE1B in activating autophagy. We found that the nucleotide binding and RNase activity of IRE1B, but not its protein kinase activity or splicing target *BZIP60*, are required for ER stress-mediated autophagy. Upon ER stress, the RNase activity of IRE1B engages in regulated IRE1-dependent decay of messenger RNA (RIDD), in which mRNAs of secreted proteins are degraded by IRE1 upon ER stress. Twelve genes most highly targeted by RIDD were tested for their role in inhibiting ER stress-induced autophagy, and 3 of their encoded proteins, AT1G66270/BGLU21 (β -glucosidase 21), AT2G16005/ROSY1/ML (MD2-related lipid recognition protein) and AT5G01870/PR-14 (pathogenesis-related protein 14), were found to inhibit autophagy upon overexpression. From these findings, IRE1B is posited to be a “licensing factor” linking ER stress to autophagy by degrading the RNA transcripts of factors that interfere with the induction of autophagy.

Introduction

Environmental stresses are a major threat to optimal productivity of plants in agricultural settings [1,2], and multiple simultaneous stresses are often encountered. Plants activate a suite of protective and adaptive mechanisms to respond to these stresses, including transcriptional, metabolic and cellular adaptations that often limit growth while increasing stress tolerance and survival [3]. One such mechanism is the upregulation of a degradation pathway termed autophagy, in which cellular materials are transferred inside the vacuole, degraded by the resident vacuolar lytic enzymes, and the breakdown products recycled [4,5]. Autophagy is active at a basal level under normal growth conditions, but is highly upregulated by a wide variety of biotic and abiotic stresses [6-14]. During nutrient deficiency autophagy functions in the recycling of materials for re-use of breakdown products to enable cell survival [7,15-18], whereas in other conditions it degrades oxidized and aggregated proteins and other macromolecules to prevent toxicity [12,19-21].

In plants, autophagy is initiated by the recruitment of ATG5 (autophagy-related protein 5) to the ER, which results in membrane expansion to form a bowl-shaped double-membrane intermediate, the phagophore [22]. Membrane expansion continues until sealing of the phagophore to generate a double-membrane vesicle termed an autophagosome [18,23], along with its release from the ER. The source of membrane for autophagosome formation is still unclear, but may derive from newly-synthesized lipids originating at the ER as well as membrane trafficked from pre-existing organelles including the ER, Golgi, endosomes and plasma membrane [24-28]. Cargo for degradation is incorporated into the forming autophagosomes either non-selectively or via binding by a receptor protein that recruits cargo by

interacting with the autophagosome membrane protein ATG8 (autophagy-related protein 8) [12,29-32]. The autophagosome outer membrane then fuses with the tonoplast, releasing the inner membrane and contents into the vacuole for degradation and recycling [4].

In *Arabidopsis thaliana*, autophagy is upregulated by ER stress, a condition in which unfolded or misfolded proteins accumulate in the ER. ER stress can be induced by agents that prevent proper folding of ER proteins, including dithiothreitol (DTT) and tunicamycin (Tm) [33,34]. Under ER stress conditions, but not other autophagy-inducing conditions such as starvation, fragments of ER are delivered to the vacuole by autophagy [6], potentially as a mechanism for disposal of aggregates of unfolded proteins that cannot be degraded by other proteolysis pathways [35]. The activation of autophagy by ER stress requires the accumulation of misfolded proteins in the ER, as demonstrated by the observation that the process can be moderated by either chemical or molecular chaperones and also can be triggered by expression of chronically misfolded proteins [36].

ER stress elicits the unfolded protein response (UPR), in which plants activate signaling pathways that result in the upregulation of genes that function in protein import and folding and in the degradation of misfolded ER proteins [34]. There are two arms of the UPR signaling pathway in *Arabidopsis*. One arm involves AT3G10800/BZIP28 (basic leucine zipper protein 28), a membrane-anchored transcription factor that is retained in the ER under normal conditions by its interaction with the molecular chaperone BiP [37]. In response to ER stress, BZIP28 is transported to the Golgi, where it is processed and released from the membrane, allowing it to move into the nucleus and activate transcription of ER stress response genes [38-40]. The second arm involves the unconventional RNA splicing factor IRE1A or B, which splices the mRNA

encoding the transcription factor AT1G42990/BZIP60 (basic leucine zipper protein 60) [41]. Unspliced *BZIP60* mRNA encodes a potentially membrane-associated protein, whereas splicing by IRE1A or B leads to loss of the transmembrane domain and the acquisition of a nuclear targeting signal. The spliced form can therefore enter the nucleus and activate transcriptional responses [41-43]. IRE1 also functions in the degradation of mRNAs encoding secretory proteins [44]. *Arabidopsis* contains 2 active IRE1 isoforms, AT2G17520/IRE1A (INOSITOL REQUIRING 1-2) and AT5G24360/IRE1B, which overlap substantially in function but also have some functional specificity [6,45,46]. We have shown previously that IRE1B is required for activation of autophagy during ER stress, whereas disruption of IRE1A has no detectable effect on autophagy [6].

IRE1 is a dual-function ribonuclease and protein kinase [33]. Point mutations in *Arabidopsis IRE1B* disrupting either its ribonuclease or kinase activities indicated that, as expected, IRE1B's ribonuclease activity is required for *BZIP60* splicing. However, IRE1B's role in linking ER stress to autophagy is independent of *BZIP60* splicing since autophagy can be induced in response to ER stress in an *Arabidopsis bzip60* mutant [6]. In animal cells, activation of autophagy upon ER stress requires the kinase activity of IRE1, which activates the MAPK8/JNK1 (mitogen-activated protein kinase 8/c-Jun N-terminal kinase 1)-MAPK9-MAPK10 pathway, in turn upregulating autophagy [47]. However, MAPK8/9/10 orthologs and components of its signaling pathway are absent in plants.

Here, we demonstrate that the ribonuclease activity of IRE1B is required for ER stress-induced autophagy in *Arabidopsis*, although independent of its normal downstream splicing target, *BZIP60* mRNA. Instead, we identify factors that inhibit the activation of autophagy,

indicating that the degradation of their mRNAs by IRE1B's RIDD activity [48] is required for the upregulation of autophagy in response to ER stress.

Results

Possible roles for IRE1B in linking ER stress to autophagy

We have previously shown that IRE1B is required for activation of autophagy during ER stress [6]; we therefore considered several possible mechanisms by which IRE1B might serve in this role (Fig. 1A). One possibility is that IRE1B splices *BZIP60* mRNA to make an active form of BZIP60 that upregulates genes required for the induction of autophagy. A second is that, through its protein kinase activity, IRE1B might autophosphorylate itself or phosphorylate other factors, initiating a signaling cascade leading to the induction of autophagy. Third, upon activation, IRE1B may oligomerize and cluster in the ER membrane, and the clustering might promote autophagy. Fourth, in response to ER stress, IRE1B might attack other mRNAs through its RIDD activity [48], with the destruction of these RNAs being required for the induction of autophagy.

BZIP60 is not required for the IRE1B-dependent induction of autophagy by ER stress

Because BZIP60 is a highly active transcription factor [49] and its mRNA is the principal target of the mRNA splicing activity of IRE1A or IRE1B [41], we reexamined the issue as to whether BZIP60 functions downstream from IRE1B in linking ER stress to autophagy. Earlier studies by Liu et al [6] address this matter using a loss-of function mutant, *bzip60-1*. In the interim, however, it is reported that *bzip60-1* is a weak allele with respect to certain phenotypes [50]. *bzip60-1* is a T-DNA mutant with an insertion in the first exon of the gene. However, an in-frame ATG downstream from the T-DNA insertion may be functional (Fig. 1B), and we

observed a modest level of partial transcript accumulation in *bzip60-1* representing the second exon, but not the full first exon (Fig. 1C). Another allele, *bzip60-3*, is an intron insertion, and we observed low level accumulation of partial transcripts representing the first exon, but not the second. The third allele, *bzip60-2*, has an insertion in the second exon and like *bzip60-3* we found modest accumulation of partial transcripts bearing the first exon. Although all 3 mutants accumulated partial transcripts, *bzip60-2* is considered to be a strong allele because the T-DNA insertion disrupts the IRE1 splice site, preventing the formation of a functional transcription factor targeted to the nucleus [50].

When autophagy was examined in the roots of the *bzip60* mutants treated with Tm, the levels of autophagy induced by ER stress in the mutants were comparable to wild-type (WT) as assessed by the formation of autophagosomes (Fig. 1D and E). We previously have demonstrated that our MDC (monodansylcadaverine) staining method reliably detects autophagosomes under our conditions in *Arabidopsis* seedling roots [51]. Thus, we concluded that in accordance with earlier findings, BZIP60 is not required for the IRE1B-dependent induction of autophagy by ER stress.

Kinase activity of IRE1B is not involved in autophagy induction upon ER stress

The second mechanism we explored was whether IRE1B might phosphorylate other proteins, initiating a signaling cascade culminating in the induction of autophagy. To test this possibility, we used site-specific mutations in the cytoplasmic domain of IRE1B to disrupt various IRE1B functions (Fig. 2A) [52]. The Asp to Ala mutation at residue 628 (D628A) is in the protein kinase catalytic domain responsible for the phospho-transfer activity of IRE1B [52-56]. In *Arabidopsis*, the D628A mutation in IRE1B knocks out its phospho-transfer activity [52]. In

other organisms, it has been shown that IRE1 undergoes auto-transphosphorylation upon activation [57-59]. In metazoans, IRE1 activates MAP3K5/ASK1 (mitogen-activated protein kinase kinase kinase 5), initiating a phosphorylation cascade leading to the activation of MAPK8/9/10 [60]. However, plant genomes do not contain MAPK8/9/10 pathway orthologs and in yeast, Ire1 is not known to phosphorylate any other cellular proteins.

The D628A mutation in IRE1B was tested for its support of UPR biomarkers and autophagy by transient expression in *Arabidopsis* leaf protoplasts derived from *ire1a ire1b* null mutant leaves. When protoplasts from *ire1a ire1b* mutant plants were transfected with a non-mutant IRE1B construct driven by the CaMV 35S promoter, expression levels of the spliced form of *BZIP60* mRNA and *AT1G09080/BIP3* (BINDING PROTEIN 3) comparable to WT were observed upon Tm treatment (Fig. 2B). To test for support of ER stress-induced autophagy, protoplasts were cotransfected with the IRE1B construct driven by the CaMV 35S promoter and the autophagosome marker GFP-AT2G45170/ATG8E, to facilitate detection of autophagosomes. As controls, protoplasts were mock-treated (DMSO treated), or were treated with the ER stress agent Tm. In mock-treated WT protoplasts, only about 15% showed evidence of autophagy, defined as protoplasts with 3 or more autophagosomes [36] (Fig. 2C). Conversely, more than 50% of WT protoplasts displayed significant levels of autophagy when treated with 5 μ g/mL Tm. In *ire1a ire1b* mutant protoplasts, mock treatment or Tm treatment resulted in the same basal level of autophagy, with little more than 15% of the protoplasts showing 3 or more autophagosomes. *ire1a ire1b* mutant protoplasts expressing non-mutant IRE1B showed similar autophagy levels as WT protoplasts.

When *ire1a ire1b* protoplasts were transfected with the kinase-dead IRE1B^{D628A} mutant driven by the CaMV 35S promoter, together with the GFP-ATG8E autophagosome marker, full restoration of ER stress-induced autophagy was observed upon Tm treatment (Fig. 2C and D). The complementation by constructs encoding IRE1B with disabled protein kinase activity indicated that the phospho-transfer activity of IRE1B is not required for ER stress to induce autophagy. Similar results were obtained with stably-transformed seedlings (Fig. 3A and B). Transgenic lines expressing the IRE1B^{D628A} mutant construct in an *ire1a ire1b* double-mutant background [52] were assessed for autophagy activity in the presence or absence of Tm by staining with MDC. These results indicate that phosphorylation of other proteins by *Arabidopsis* IRE1B, if it does occur, is not required for the induction of autophagy by ER stress.

The ribonuclease activity of IRE1B is required for autophagy induction upon ER stress

The RNase activity of plant IRE1B mediates the splicing of *BZIP60* mRNA and supports its RIDD activity. The RNase domain of IRE1B is located near its C terminus, and the Asn to Ala mutation at residue 820 (N820A) in the catalytic site inactivates its endonuclease activity [52]. The effect of the IRE1B^{N820A} mutation on splicing was demonstrated by expressing the construct driven by a 35S promoter in *ire1a ire1b* protoplasts or transgenic plants and testing by RT-PCR for spliced *BZIP60* mRNA (*BZIP60s*, Fig. 2B and Fig. 3C, respectively). RNA splicing activity was disrupted in the *ire1a ire1b* double knockout mutant, and expression of IRE1B^{N820A} failed to complement *ire1a ire1b* protoplasts, while expression of the WT protein rescued splicing activity. Consistent with this, *BIP3* expression was upregulated by Tm in *ire1a ire1b* protoplasts expressing WT IRE1B but not in protoplasts expressing the IRE1B^{N820A} mutant (Fig. 2B).

As above, the IRE1B^{N820A} construct was transfected into *ire1a ire1b* protoplasts and tested for its ability to restore ER stress-induced autophagy. Unlike the IRE1B^{D628A} mutant, the RNase-dead construct failed to complement the double *ire1a ire1b* mutant and restore ER stress-induced autophagy in transient assays with protoplasts (Fig. 2C and D) and in stably transformed seedlings (Fig. 3A and B). This suggested that the RNase activity of IRE1B is necessary for activation of autophagy upon ER stress.

In yeast, nucleotide binding to Ire1, but not its phospho-transfer activity, is required to activate Ire1's RNase activity [61]. For example, Papa et al. [61] show that a form of Ire1 with an expanded nucleotide-binding pocket is activated by an ATP mimic and kinase inhibitor, 1NM-PP1. Other studies demonstrated that the RNase activity of wild-type Ire1 can also be activated *in vitro* by other kinase inhibitors, such as APY29 and sunitinib [62]. The binding of ATP-mimetic ligands to the nucleotide-binding site of human ERN1/IRE1a promotes its oligomerization, which, in turn, activates its RNase activity. Thus, ligand occupancy in the nucleotide-binding site drives the conformational changes activating ERN1/IRE1a [63].

In *Arabidopsis*, the effect of the Asp to Asn at residue 608 (D608N) and Lys to Asn at residue 610 (K610N) double mutation in IRE1B, blocking nucleotide binding, on *BZIP60* mRNA splicing was demonstrated by expressing the construct driven by a 35S promoter in *ire1a ire1b* protoplasts and again testing by RT-PCR for the spliced form of *BZIP60* mRNA. Like the N820A mutant, the IRE1B^{D608NK610N} double mutant failed to complement the splicing of *BZIP60* mRNA in *ire1a ire1b* protoplasts (Fig. 2B). Thus, nucleotide binding is needed to activate IRE1B mRNA splicing function [52].

We therefore determined whether a functional nucleotide-binding site in IRE1B was required for ER stress induction of autophagy, using the IRE1B^{D608N,K610N} double mutant. In the transient expression system (Fig. 2C and D) and in stably transformed seedlings (Fig. 3A and B), D608N K610N double mutants failed to restore ER stress-induced autophagy to the *ire1a ire1b* null mutant. Thus, we reason that nucleotide binding to IRE1B is needed to activate IRE1B's RNase activity in order for IRE1B to link ER stress to autophagy.

IRE1B clustering is not sufficient for autophagy induction upon ER stress

Nucleotide binding activates IRE1 by altering its conformation and promoting its oligomerization or clustering [59,64]. Oligomerization is vital to IRE1's function because it promotes transphosphorylation of IRE1 monomers and creates surfaces for the binding of the target mRNA [62]. Yeast Ire1 and mammalian ERN1/IRE1a undergo clustering in response to stress [65], and so we assessed whether IRE1B clusters in *Arabidopsis*, and whether clustering promotes autophagy. We generated an IRE1B-YFP fusion construct and demonstrated that it is biologically active, as shown by its support for the splicing of *BZIP60* mRNA in response to Tm (Fig. 4A). When transfected into protoplasts, IRE1B-YFP was distributed in protoplasts in a pattern mostly coinciding with an ER marker, as expected (Fig. 4B). When the protoplasts were treated with Tm, we observed pronounced clustering of IRE1B-YFP (Fig. 4C and D). A similar YFP fusion was generated with the RNase dead mutant IRE1B to make IRE1B^{N820A}-YFP. This construct was not biologically active as demonstrated by its failure to splice *BZIP60* mRNA in response to stress (Fig. 4A). When the RNase mutant fusion construct was introduced into protoplasts, it clustered normally in response to treatment with Tm (Fig. 4C and D). Because the

RNase-dead mutant clustered normally, but did not support ER stress induced autophagy, this fails to implicate IRE1B clustering as a key event in ER stress-induced autophagy.

RIDD genes negatively regulate induction of autophagy upon ER stress

Having eliminated 3 mechanisms by which IRE1B might mediate the link between ER stress and autophagy, we explored the possibility that the RIDD activity of IRE1B is involved in this role. RIDD targets in *Arabidopsis* have been identified by Mishiba et al. [44] and Deng et al. [52] as genes with expression that declines in response to ER stress in WT, but not in *ire1a ire1b* null mutants. We performed a transcriptomic analysis (Gene Expression Omnibus database, accession number GSE99576) and identified the top 12 genes that were most highly spared from downregulation in an *ire1a ire1b* null mutant compared to WT and also in the *ire1b* mutant alone compared to WT (Table 1). The most vulnerable targets are mRNA transcripts encoding secretory proteins, translated on ribosomes associated with the ER membrane.

We interpret the involvement of RIDD in mediating ER-stress induced autophagy to mean that certain RNA transcripts have to be degraded by IRE1B for ER stress to induce autophagy. Therefore, we overexpressed each of the top RIDD targets to determine whether they would interfere with ER stress-induced autophagy in a WT background. cDNAs representing the RIDD target mRNAs were introduced into *Arabidopsis* protoplasts together with the autophagosome marker GFP-ATG8E, and autophagosome production in response to treatment with Tm was assessed. We found that the expression of cDNAs representing AT1G66270/BGLU21 (β -glucosidase 21), AT5G01870/PR-14 (pathogenesis-related protein 14) and AT2G16005/ROSY1/ML (interactor of synaptotagmin 1, also known as MD2-related lipid recognition protein) were the most disruptive to ER stress-induced autophagy (Fig. 5A).

It is possible that either the RNA or the protein that it encodes might interfere with the induction of autophagy. Therefore, we generated mutant forms of *BGLU21*, *PR-14* and *ROSY1/ML* in which the initiating AUG was knocked out, and tested them for their ability to disrupt ER stress-induced autophagy (Fig. 5B). We found that none of the mutants interfered with ER stress-induced autophagy, indicating that the protein product encoded by the RNA, rather than the RNA itself, was most likely responsible for the interference.

To confirm that the inhibition of autophagy by the RIDD targets is specific to ER stress, cDNAs representing the RIDD target mRNAs were introduced into *Arabidopsis* protoplasts together with the autophagosome marker GFP-ATG8E, and the protoplasts were subjected to sucrose starvation as an alternative well-characterized condition that activates autophagy [28]. None of the mutants had an effect on starvation-induced autophagy (Fig. 5C). Taken together, our results suggest that *BGLU21*, *PR-14* and *ROSY1/ML* specifically inhibit ER stress-induced autophagy and that *IRE1B* relieves their inhibition by degrading their RNA transcripts.

Discussion

Autophagy is generally regarded as a cell survival or renewal response that functions by turning over cellular contents. Autophagy in response to ER stress is thought to degrade damaged ER components since ER stress induces the formation of autophagosomes that include ER membranes and their contents. We showed previously in *Arabidopsis* that *IRE1B* is required for activation of autophagy specifically during ER stress [6]. Here, we considered possible mechanisms by which *IRE1B* might function in autophagy, and distinguished between them by knocking out *BZIP60* and by selectively disabling various *IRE1B* activities. We eliminated several possibilities, including the involvement of *BZIP60*, a protein phosphorylation cascade

initiated by the protein kinase activity of IRE1B, and the stress-induced clustering of IRE1B. Loss of BZIP60 had no effect on autophagy, nor did a D628A mutation in IRE1B, which inhibits its phospho-transfer activity. By contrast, a N820A mutation in the RNase domain of IRE1B effectively blocked ER stress-induced autophagy, demonstrating the essential role of the RNase activity. In addition, disruption of the nucleotide-binding site in IRE1B by the IRE1B^{D608N,K610N} double mutation had the same effect. The likely explanation for this is that nucleotide binding, but not phospho-transfer, is required to activate the RNase activity of IRE1 [61].

Because IRE1B's RNase activity, but not BZIP60, is required to link ER stress to autophagy, it suggests that the RIDD activity and not the RNA splicing activity of IRE1B is important in making the connection. In view of these findings, we assessed whether the RNA degradation that links ER stress to autophagy is global or selective with respect to the transcripts degraded. To address this issue, we tested the top 12 RIDD targets individually for their ability to disrupt ER stress-induced autophagy. The transcripts from 3 genes negatively regulated ER stress-induced autophagy, *BGLU21*, *ROSY1/ML* and *PR-14*, whereas the others had no effect. Knocking out the major open reading frames in these transcripts demonstrated that the proteins encoded by the transcripts, and not the RNAs themselves, were critical for inhibiting autophagy. The 3 genes that enable ER stress-induced autophagy are not well described, although they allegedly have different functions, all relating to the ER. *BGLU21* is a member of the β -glucosidase family, a major component of ER bodies [66]. ER bodies are large spindle-shaped structures that are contiguous with the ER and are produced constitutively in seedlings, but are wound-induced in rosette leaves [67], where they are thought to function in defense responses [68]. Upon encountering stresses such as salt stress, ER bodies fuse with the vacuole, delivering

stress-response and cell death components into the vacuole [66]. BGLU21 itself is not wound inducible, but is a component of ER body contents. β -glucosidase family members have been implicated in ER body formation; the *Arabidopsis nail* knockout mutant downregulates AT3G09260/ β -glucosidase 23 and lacks constitutive ER bodies, while another mutant with downregulation of AT1G52400/ β -glucosidase 18 prevents the formation of wound inducible ER bodies [69]. BGLU21 is closely related to β -glucosidase 23, and whereas single loss-of-function *bglu21* mutants have no ER body phenotype, they synergize with β -glucosidase 23 mutants in reducing ER bodies [70], suggesting that these proteins work together in ER body formation. It is not known whether glucosidases are recruited into ER bodies as they form or whether they assemble ER bodies. In either case, the β -glucosidases appear to have a role in the assembly of large membrane-bound structures such as ER bodies. Autophagosome formation also requires large quantities of membrane components. Under stress conditions, whether ER body glucosidases such as BGLU21 compete with assembly of other vesicular structures from the ER, such as autophagosomes, needs further investigation.

The other 2 genes that negatively act upon ER stress-induced autophagy encode proteins that interact with lipids. AT2G16005 is the gene ID (as assigned by The Arabidopsis Information Resource) corresponding to an MD2-related lipid recognition domain protein (ROSY1/ML), and proteins with this domain often bind and/or transport lipids or sterols [71]; ROSY1 binds stigmasterol and phosphoethanolamines [72]. The third gene identified, AT5G01870, is a pathogenesis related protein (PR-14) related to lipid transfer proteins, and is unrelated in sequence to ROSY1/ML proteins. Lipid transfer proteins provide non-vesicular means by which lipids can be transferred from the ER to other organelles. Autophagosome formation involves the

lipidation of Atg8 (or members of its protein family in mammals), achieved by its coupling to phosphatidylethanolamine [73], and also requires the recruitment of lipids to the newly-forming autophagosome membrane. It is possible that these lipid-interacting proteins negatively regulate autophagy by competing or interfering with the lipidation of autophagic factors or by disrupting the recruitment or assembly of lipid components in the formation of autophagosomes.

An important question is whether the transcripts of these genes are the incidental or intended targets of IRE1B. In our work and that of Mishiba et al. [44] in *Arabidopsis*, the major RIDD targets are RNA transcripts encoding proteins that enter the endomembrane system. These transcripts are loaded onto ribosomes and serve as templates for the synthesis of proteins undergoing cotranslational insertion into the ER. During stress, the degradation of RNAs encoding secreted proteins by IRE1 may reduce the load of proteins in the ER requiring folding. The slowing of translation during ER stress is well documented in metazoans in which EIF2AK3/PERK (eukaryotic translation initiation factor 2-alpha kinase 3/protein kinase R-like endoplasmic reticulum kinase) phosphorylates and inactivates EIF2S1/eIF2a, which in turn reduces translation initiation [74]. *Arabidopsis* has no currently identifiable EIF2AK3/PERK ortholog, and instead, RIDD may serve to slow translation during ER stress.

If the role of IRE1B in regulating ER stress-induced autophagy is to eliminate factors that interfere with the induction of autophagy, then what actually induces autophagy in response to stress? Is it simply the elimination of these negative regulators that leads to the induction of autophagy? Or does IRE1B function as a “licensing factor” that renders cells competent to respond to positive induction signals? The problem is similar to the induction of autophagy in

response to metabolic deprivation. Future work is needed to characterize the mechanism by which IRE1B regulates autophagy upon ER stress.

Materials and Methods

Plant materials and growth conditions

All lines used in this study were in the Columbia-0 (Col-0) background. Seeds were sterilized in 33% (v:v) bleach with 0.1% (v:v) Triton X-100 (Fisher Scientific, BP151) for 20 min, followed by washing with sterile water at least 5 times. After being stratified in the dark at 4°C for at least 48 h, sterilized seeds were plated and germinated on ½ strength MS solid medium (Murashige & Skoog vitamin and salt mixture [Caisson Laboratories, MSP01], 0.5% [w:v] sucrose [Sigma-Aldrich, S0389], 2.4 mM MES [Sigma-Aldrich, M3671], pH 5.7, and 0.6% [w:v] phytoagar [Caisson Laboratories, PTP01]). Unless otherwise noted, plants were grown at 22°C in long-day conditions (16 h light/8 h dark). *bip60-1*, *bzip60-2*, *ire1b* mutants, as well as *ire1a ire1b* T-DNA insertion mutants and transgenic lines harboring various IRE1B point mutants were described previously [52]. The *bzip60-3* (GABI-Kat, 326A12) mutant was obtained from the Nottingham *Arabidopsis* Stock Centre and GABI-Kat [75], and homozygous plants were genotyped using gene specific primers and the T-DNA specific primer pAC161-LB1. Primers used in this study are listed in Table S1.

MDC staining and microscopy analyses

MDC staining of Tm treated *Arabidopsis* roots was described previously [6,76]. Seven-day-old seedlings were treated with DMSO (as the control; Fisher Scientific, D128) or 5 µg/mL Tm (Sigma-Aldrich, T7765) in 1/2 MS liquid medium for 6 h, followed by incubation with 0.05 mM

MDC (Sigma-Aldrich, 30432) for 10 min in the dark. After 3 brief washes with phosphate-buffered saline (8% [w:v] NaCl [Sigma-Aldrich, S3014], 0.2% [w:v] KCl [Fisher Scientific, BP366], 1.4% [w:v] Na₂HPO₄ [Sigma-Aldrich, S5136], 0.24% [w:v] KH₂PO₄ [Fisher Scientific, P285], pH 7.4), samples were observed by epifluorescence microscopy (Carl Zeiss Axio Imager.A2, Carl Zeiss, Jena, Germany), and a 4', 6-diamidino-2-phenylindole (DAPI)-specific filter was used to visualize MDC fluorescence. For confocal microscopy analysis, samples were observed with a Leica SP5 X MP confocal microscope (Leica Microsystems, Wetzlar, Germany) with excitation and emission at 520 nm and 550 nm for YFP, 488 nm and 509 nm for GFP, and 575 nm and 650 nm for mCherry.

Vector construction

For cloning the RIDD target genes, PCR fragments were first amplified with gene-specific primers (Table S1) from Col-0 cDNA using PfuUltra II Fusion HS DNA Polymerase (Agilent, 600670-51). Primers for generation of *mBGLU21*, *mROSY1/mML* and *mPR-14* contained the desired mutations as indicated in Table S1. PCR fragments of *BGLU21*, *VSP1*, *PRX34*, *PROX-P*, *PR-14*, *CTS1*, *GLH19*, *ROSY1/ML*, *PROX-S*, *mBGLU21*, *mROSY1/mML* and *mPR-14* were digested with Bam HI and SalI, and *PR4* and *PME41* fragments were digested with BamHI and XhoI. After being cleaned with a QIAquick Gel Extraction Kit (QIAGEN, 28704), fragments were inserted using Ligation Kit Mighty Mix (Takara Bio USA, 6023) into a pCambia2301 vector [77], which contains a double 35S promoter to drive expression and a downstream NOS terminator.

For constructs for analysis of IRE1B clustering, PCR fragments of IRE1B and IRE1B^{N820A} were amplified directly from the constructs in our former study [52], digested with

SmaI and SpeI, and inserted into a modified pCambia1300S-YFP vector [78], which contains a double 35S promoter and NOS terminator [78].

Subcellular localization analyses

Protoplast isolation and transformation were previously described [79]. A protoplast was considered to have active autophagy if it contained 3 or more autophagosomes [36]. For analysis of IRE1B-YFP and IRE1B^{N820A}-YFP clustering in response to ER stress, 20 µg plasmid (GenElute HP Plasmid Maxiprep Kit; Sigma-Aldrich, NA0310-1KT) at a concentration of 1 µg/µL was introduced into WT protoplasts. After dark incubation for 12 h, protoplasts were treated with DMSO (as control) or with 5 µg/mL Tm for 6 h in 6-well COSTAR Cell Culture Plates (Corning Incorporated, 3506). For colocalization analyses, WT protoplasts were cotransformed with 20 µg of IRE1B-YFP and 20 µg ER-mCherry (TAIR stock number CD3-959) or Golgi-mCherry (TAIR stock number CD3-967) [80] and incubated in the dark for 12 h before observation by confocal microscopy. For visualization of autophagosomes, GFP-ATG8E was introduced alone or together with various IRE1B constructs. Images were taken using a Leica SP5 X MP confocal microscope using a ×63 Leica oil immersion objective, with excitation and emission at 520 nm and 550 nm for YFP, 488 nm and 509 nm for GFP, and 575 nm and 650 nm for mCherry.

RNA isolation and RT-PCR analyses

RNA samples were extracted using an RNeasy Plant Mini Kit (QIAGEN, 74904), according to the manufacturer's instructions. Synthesis of the first strand cDNA was performed with an iScript™ cDNA Synthesis Kit (BioRad, 1708891). RT-PCR was performed using a C1000

Touch Thermal Cycler (Bio-Rad Laboratories, Hercules, CA, USA) in 8-well strip PCR tubes. Primers used in RT-PCR are listed in Table S1.

RNA-seq analysis

Seeds from WT, *ire1b* and *ire1a ire1b* genotypes were germinated and seedlings grown vertically on 100 mm × 100 mm square plates (Fisher Scientific, FB0875711A) on 1/2 MS medium for 7 days. Seedlings of similar size were treated with DMSO (as the control) or with 5 µg/mL Tm in 6-well cell culture plates with liquid 1/2 MS-0 media for 6 h. Samples were harvested by removal of the liquid and immediately ground into powder in liquid nitrogen. Total RNA was extracted using an RNeasy Plant Mini Kit (QIAGEN, 74904). Quality and quantity of RNA were assessed using a Nanodrop1000 spectrophotometer (Thermo Fisher Scientific, Wilmington, DE, USA), and samples with a ratio of absorbance for both OD 260/230 and OD 260/280 > 1.8 were sent for RNA sequencing by BGI-Hong Kong. RNA-seq libraries were prepared and subjected to paired end sequencing with read length 250 base pairs. Read counts in each library were normalized using the TMM method, which is the weighted trimmed mean of M-values proposed by Robinson and Oshlack [81], where the weights are from the delta method on Binomial data. Sequences were aligned to the *Arabidopsis* TAIR10 genome, using STAR (version 2.4.0). The read count for each annotated gene was calculated by htseq-count (version 0.6.0 with parameters “-t mRNA -m intersection-nonempty --stranded no”). Differential gene expression between samples was assessed using negative-binomial generalized-linear models with DESeq2 tools [82]. Significant differentially expressed genes were defined as those with a false discovery rate (*Q* value) < 0.01. The raw data and gene read counts have been deposited in the Gene Expression Omnibus database under accession number GSE99576.

Statistical analysis

All experiments in this study were performed with at least 3 biological replicates. Data were subjected to a Student's t test and differences with a *P* value of < 0.05 were considered statistically significant.

Acknowledgements

This work was supported by the National Science Foundation under Grant IOS 1353867 to DCB and SHH.

References

- [1] Sah SK, Reddy KR, Li J. Abscisic Acid and Abiotic Stress Tolerance in Crop Plants. *Front Plant Sci.* 2016;7:571. Epub 2016/05/21.
- [2] Boyer J. Plant Productivity and Environment. *Science.* 1982;218:443-8.
- [3] Cramer GR, Urano K, Delrot S, Pezzotti M, Shinozaki K. Effects of abiotic stress on plants: a systems biology perspective. *BMC Plant Biol.* 2011;11:163. Epub 2011/11/19.
- [4] Yang X, Bassham DC. New Insight into the Mechanism and Function of Autophagy in Plant Cells. *Int Rev Cell Mol Biol.* 2015;320:1-40. Epub 2015/11/29.
- [5] Michaeli S, Galili G, Genschik P, Fernie AR, Avin-Wittenberg T. Autophagy in Plants--What's New on the Menu? *Trends Plant Sci.* 2016;21:134-44. Epub 2015/11/26.
- [6] Liu Y, Burgos JS, Deng Y, Srivastava R, Howell SH, Bassham DC. Degradation of the endoplasmic reticulum by autophagy during endoplasmic reticulum stress in Arabidopsis. *Plant Cell.* 2012;24:4635-51. Epub 2012/11/24.
- [7] Xiong Y, Contento AL, Bassham DC. AtATG18a is required for the formation of autophagosomes during nutrient stress and senescence in Arabidopsis thaliana. *Plant J.* 2005;42:535-46.
- [8] Liu Y, Xiong Y, Bassham DC. Autophagy is required for tolerance of drought and salt stress in plants. *Autophagy.* 2009;5:954-63. Epub 2009/07/10.
- [9] Larson ER, Domozych DS, Tierney ML. SNARE VTI13 plays a unique role in endosomal trafficking pathways associated with the vacuole and is essential for cell wall organization and root hair growth in Arabidopsis. *Ann Bot.* 2014;114:1147-59. Epub 2014/04/17.

- [10] Li F, Chung T, Pennington JG, Federico ML, Kaeppler HF, Kaeppler SM, Otegui MS, Vierstra RD. Autophagic recycling plays a central role in maize nitrogen remobilization. *Plant Cell*. 2015;27:1389-408. Epub 2015/05/07.
- [11] Yoshimoto K, Hanaoka H, Sato S, Kato T, Tabata S, Noda T, Ohsumi Y. Processing of ATG8s, ubiquitin-like proteins, and their deconjugation by ATG4s are essential for plant autophagy. *Plant Cell*. 2004;16:2967-83. Epub 2004/10/21.
- [12] Zhou J, Wang J, Cheng Y, Chi YJ, Fan B, Yu JQ, Chen Z. NBR1-Mediated Selective Autophagy Targets Insoluble Ubiquitinated Protein Aggregates in Plant Stress Responses. *PLoS Genet*. 2013;9:e1003196.
- [13] Zhou J, Wang J, Yu JQ, Chen Z. Role and regulation of autophagy in heat stress responses of tomato plants. *Front Plant Sci*. 2014;5:174.
- [14] Kwon SI, Cho HJ, Kim SR, Park OK. The Rab GTPase RabG3b positively regulates autophagy and immunity-associated hypersensitive cell death in Arabidopsis. *Plant Physiol*. 2013;161:1722-36. Epub 2013/02/14.
- [15] Uemura T, Ueda T, Ohniwa RL, Nakano A, Takeyasu K, Sato MH. Systematic analysis of SNARE molecules in Arabidopsis: Dissection of the post-Golgi network in plant cells. *Cell Struct Funct*. 2004;29:49-65.
- [16] Moriyasu Y, Ohsumi Y. Autophagy in tobacco suspension-cultured cells in response to sucrose starvation. *Plant Physiol*. 1996;111:1233-41.
- [17] Gullapalli A, Wolfe B, Griffin C, Magnuson T, Trejo J. An essential role for SNX1 in lysosomal sorting of protease-activated receptor-1: evidence for retromer-, Hrs-, and Tsg101-independent functions of sorting nexins. *Mol Biol Cell*. 2006;17:1228-38.

- [18] Aubert S, Gout E, Bligny R, MartyMazars D, Barrieu F, Alabouvette J, Marty F, Douce R. Ultrastructural and biochemical characterization of autophagy in higher plant cells subjected to carbon deprivation: Control by the supply of mitochondria with respiratory substrates. *J Cell Biol.* 1996;133:1251-63.
- [19] Xiong Y, Contento AL, Nguyen PQ, Bassham DC. Degradation of oxidized proteins by autophagy during oxidative stress in Arabidopsis. *Plant Physiol.* 2007;143:291-9. Epub 2006/11/14.
- [20] Zhou J, Zhang Y, Qi J, Chi Y, Fan B, Yu JQ, Chen Z. E3 ubiquitin ligase CHIP and NBR1-mediated selective autophagy protect additively against proteotoxicity in plant stress responses. *PLoS Genet.* 2014;10:e1004116.
- [21] Zhu JH, Gong ZZ, Zhang CQ, Song CP, Damsz B, Inan G, Koiwa H, Zhu JK, Hasegawa PM, Bressan RA. OSM1/SYP61: A syntaxin protein in Arabidopsis controls abscisic acid-mediated and non-abscisic acid-mediated responses to abiotic stress. *Plant Cell.* 2002;14:3009-28.
- [22] Le Bars R, Marion J, Le Borgne R, Satiat-Jeunemaitre B, Bianchi MW. ATG5 defines a phagophore domain connected to the endoplasmic reticulum during autophagosome formation in plants. *Nat Commun.* 2014;5:4121. Epub 2014/06/21.
- [23] Rose TL, Bonneau L, Der C, Marty-Mazars D, Marty F. Starvation-induced expression of autophagy-related genes in Arabidopsis. *Biol Cell.* 2006;98:53-67.
- [24] Lamb CA, Yoshimori T, Tooze SA. The autophagosome: origins unknown, biogenesis complex. *Nat Rev Mol Cell Biol.* 2013;14:759-74. Epub 2013/11/10.

- [25] Chan SN, Tang BL. Location and membrane sources for autophagosome formation - from ER-mitochondria contact sites to Golgi-endosome-derived carriers. *Mol Membr Biol*. 2013;30:394-402. Epub 2013/11/02.
- [26] Puri C, Renna M, Bento CF, Moreau K, Rubinsztein DC. Diverse autophagosome membrane sources coalesce in recycling endosomes. *Cell*. 2013;154:1285-99. Epub 2013/09/17.
- [27] Ge L, Melville D, Zhang M, Schekman R. The ER-Golgi intermediate compartment is a key membrane source for the LC3 lipidation step of autophagosome biogenesis. *eLife*. 2013;2:e00947. Epub 2013/08/10.
- [28] Contento AL, Kim SJ, Bassham DC. Transcriptome profiling of the response of *Arabidopsis* suspension culture cells to Suc starvation. *Plant Physiol*. 2004;135:2330-47.
- [29] Floyd BE, Morriss SC, Macintosh GC, Bassham DC. What to eat: evidence for selective autophagy in plants. *J Int Plant Biol*. 2012;54:907-20. Epub 2012/10/11.
- [30] Zientara-Rytter K, Lukomska J, Moniuszko G, Gwozdecki R, Surowiecki P, Lewandowska M, Liszewska F, Wawrzynska A, Sirko A. Identification and functional analysis of Joka2, a tobacco member of the family of selective autophagy cargo receptors. *Autophagy*. 2011;7:1145-58. Epub 2011/06/15.
- [31] Vanoosthuysse V, Tichtinsky G, Dumas C, Gaude T, Cock J. Interaction of calmodulin, a sorting nexin and kinase-associated protein phosphatase with the *Brassica oleracea* S locus receptor kinase. *Plant Physiol*. 2003;133:919-29.
- [32] Marshall RS, Li F, Gemperline DC, Book AJ, Vierstra RD. Autophagic Degradation of the 26S Proteasome Is Mediated by the Dual ATG8/Ubiquitin Receptor RPN10 in *Arabidopsis*. *Mol Cell*. 2015;58:1053-66.

- [33] Howell SH. Endoplasmic reticulum stress responses in plants. *Annu Rev Plant Biol.* 2013;64:477-99. Epub 2013/01/22.
- [34] Liu JX, Howell SH. Managing the protein folding demands in the endoplasmic reticulum of plants. *New Phytol.* 2016;211:418-28. Epub 2016/03/19.
- [35] Liu Y, Bassham DC. Degradation of the endoplasmic reticulum by autophagy in plants. *Autophagy.* 2013;9:622-3. Epub 2013/01/31.
- [36] Yang X, Srivastava R, Howell SH, Bassham DC. Activation of autophagy by unfolded proteins during endoplasmic reticulum stress. *Plant J.* 2015;85:83-95.
- [37] Srivastava R, Deng Y, Shah S, Rao AG, Howell SH. BINDING PROTEIN Is a master regulator of the endoplasmic reticulum stress sensor/transducer bZIP28 in Arabidopsis. *Plant Cell.* 2013;25:1416-29. Epub 2013/04/30.
- [38] Liu JX, Srivastava R, Che P, Howell SH. An endoplasmic reticulum stress response in Arabidopsis is mediated by proteolytic processing and nuclear relocation of a membrane-associated transcription factor, bZIP28. *Plant Cell.* 2007;19:4111-9. Epub 2007/12/25.
- [39] Tajima H, Iwata Y, Iwano M, Takayama S, Koizumi N. Identification of an Arabidopsis transmembrane bZIP transcription factor involved in the endoplasmic reticulum stress response. *Biochem Biophys Res Comm.* 2008;374:242-7.
- [40] Gao H, Brandizzi F, Benning C, Larkin RM. A membrane-tethered transcription factor defines a branch of the heat stress response in Arabidopsis thaliana. *Proc Natl Acad Sci USA.* 2008;105:16398-403. Epub 2008/10/14.
- [41] Deng Y, Humbert S, Liu JX, Srivastava R, Rothstein SJ, Howell SH. Heat induces the splicing by IRE1 of a mRNA encoding a transcription factor involved in the unfolded protein response in Arabidopsis. *Proc Natl Acad Sci USA.* 2011;108:7247-52. Epub 2011/04/13.

- [42] Chen Y, Brandizzi F. AtIRE1A/AtIRE1B and AGB1 independently control two essential unfolded protein response pathways in Arabidopsis. *Plant J.* 2012;69:266-77. Epub 2011/09/15.
- [43] Nagashima Y, Mishiba K, Suzuki E, Shimada Y, Iwata Y, Koizumi N. Arabidopsis IRE1 catalyses unconventional splicing of bZIP60 mRNA to produce the active transcription factor. *Sci Reports.* 2011;1:29. Epub 2012/02/23.
- [44] Mishiba K, Nagashima Y, Suzuki E, Hayashi N, Ogata Y, Shimada Y, Koizumi N. Defects in IRE1 enhance cell death and fail to degrade mRNAs encoding secretory pathway proteins in the Arabidopsis unfolded protein response. *Proc Natl Acad Sci USA.* 2013;110:5713-8. Epub 2013/03/20.
- [45] Koizumi N, Martinez IM, Kimata Y, Kohno K, Sano H, Chrispeels MJ. Molecular characterization of two Arabidopsis Ire1 homologs, endoplasmic reticulum-located transmembrane protein kinases. *Plant Physiol.* 2001;127:949-62.
- [46] Moreno AA, Mukhtar MS, Blanco F, Boatwright JL, Moreno I, Jordan MR, Chen Y, Brandizzi F, Dong X, Orellana A, Pajeroska-Mukhtar KM. IRE1/bZIP60-mediated unfolded protein response plays distinct roles in plant immunity and abiotic stress responses. *PloS One.* 2012;7:e31944. Epub 2012/02/24.
- [47] Ogata M, Hino S, Saito A, Morikawa K, Kondo S, Kanemoto S, Murakami T, Taniguchi M, Tanii I, Yoshinaga K, Shiosaka S, Hammarback JA, Urano F, Imaizumi K. Autophagy is activated for cell survival after endoplasmic reticulum stress. *Mol Cell Biol.* 2006;26:9220-31. Epub 2006/10/13.
- [48] Hollien J, Lin JH, Li H, Stevens N, Walter P, Weissman JS. Regulated Ire1-dependent decay of messenger RNAs in mammalian cells. *J Cell Biol.* 2009;186:323-31. Epub 2009/08/05.

- [49] Iwata Y, Koizumi N. An Arabidopsis transcription factor, AtbZIP60, regulates the endoplasmic reticulum stress response in a manner unique to plants. *Proc Natl Acad Sci USA*. 2005;102:5280-5.
- [50] Zhang L, Chen H, Brandizzi F, Verchot J, Wang A. The UPR branch IRE1-bZIP60 in plants plays an essential role in viral infection and is complementary to the only UPR pathway in yeast. *PLoS Genet*. 2015;11:e1005164. Epub 2015/04/16.
- [51] Floyd BE, Morriss SC, MacIntosh GC, Bassham DC. Evidence for autophagy-dependent pathways of rRNA turnover in Arabidopsis. *Autophagy*. 2015;11:2199-212.
- [52] Deng Y, Srivastava R, Howell SH. Protein kinase and ribonuclease domains of IRE1 confer stress tolerance, vegetative growth, and reproductive development in Arabidopsis. *Proc Natl Acad Sci USA*. 2013;110:19633-8. Epub 2013/10/23.
- [53] Nishitoh H, Saitoh M, Mochida Y, Takeda K, Nakano H, Rothe M, Miyazono K, Ichijo H. ASK1 is essential for JNK/SAPK activation by TRAF2. *Mol Cell*. 1998;2:389-95. Epub 1998/10/17.
- [54] Matsukawa J, Matsuzawa A, Takeda K, Ichijo H. The ASK1-MAP kinase cascades in mammalian stress response. *J Biochem*. 2004;136:261-5.
- [55] Tabas I, Ron D. Integrating the mechanisms of apoptosis induced by endoplasmic reticulum stress. *Nature Cell Biol*. 2011;13:184-90. Epub 2011/03/03.
- [56] Shiizaki S, Naguro I, Ichijo H. Activation mechanisms of ASK1 in response to various stresses and its significance in intracellular signaling. *Adv Biol Regul*. 2013;53:135-44.
- [57] Ali MM, Bagratuni T, Davenport EL, Nowak PR, Silva-Santisteban MC, Hardcastle A, McAndrews C, Rowlands MG, Morgan GJ, Aherne W, Collins I, Davies FE, Pearl LH. Structure

of the Ire1 autophosphorylation complex and implications for the unfolded protein response. *EMBO J.* 2011;30:894-905. Epub 2011/02/15.

[58] Lee KP, Dey M, Neculai D, Cao C, Dever TE, Sicheri F. Structure of the dual enzyme Ire1 reveals the basis for catalysis and regulation in nonconventional RNA splicing. *Cell.* 2008;132:89-100. Epub 2008/01/15.

[59] Shamu CE, Walter P. Oligomerization and phosphorylation of the Ire1p kinase during intracellular signaling from the endoplasmic reticulum to the nucleus. *EMBO J.* 1996;15:3028-39.

[60] Ichijo H, Nishida E, Irie K, ten Dijke P, Saitoh M, Moriguchi T, Takagi M, Matsumoto K, Miyazono K, Gotoh Y. Induction of apoptosis by ASK1, a mammalian MAPKKK that activates SAPK/JNK and p38 signaling pathways. *Science.* 1997;275:90-4. Epub 1997/01/03.

[61] Papa FR, Zhang C, Shokat K, Walter P. Bypassing a kinase activity with an ATP-competitive drug. *Science.* 2003;302:1533-7. Epub 2003/10/18.

[62] Korennykh AV, Egea PF, Korostelev AA, Finer-Moore J, Zhang C, Shokat KM, Stroud RM, Walter P. The unfolded protein response signals through high-order assembly of Ire1. *Nature.* 2009;457:687-93. Epub 2008/12/17.

[63] Mendez AS, Alfaro J, Morales-Soto MA, Dar AC, McCullagh E, Gotthardt K, Li H, Acosta-Alvear D, Sidrauski C, Korennykh AV, Bernales S, Shokat KM, Walter P. Endoplasmic reticulum stress-independent activation of unfolded protein response kinases by a small molecule ATP-mimic. *eLife.* 2015;4.

[64] Kimata Y, Ishiwata-Kimata Y, Ito T, Hirata A, Suzuki T, Oikawa D, Takeuchi M, Kohno K. Two regulatory steps of ER-stress sensor Ire1 involving its cluster formation and interaction with unfolded proteins. *J Cell Biol.* 2007;179:75-86. Epub 2007/10/10.

[65] Li H, Korennykh AV, Behrman SL, Walter P. Mammalian endoplasmic reticulum stress sensor IRE1 signals by dynamic clustering. *Proc Natl Acad Sci USA*. 2010;107:16113-8. Epub 2010/08/28.

[66] Hayashi Y, Yamada K, Shimada T, Matsushima R, Nishizawa NK, Nishimura M, Hara-Nishimura I. A proteinase-storing body that prepares for cell death or stresses in the epidermal cells of Arabidopsis. *Plant Cell Physiol*. 2001;42:894-9.

[67] Matsushima R, Hayashi Y, Kondo M, Shimada T, Nishimura M, Hara-Nishimura I. An endoplasmic reticulum-derived structure that is induced under stress conditions in Arabidopsis. *Plant Physiol*. 2002;130:1807-14.

[68] Nakano RT, Pislewska-Bednarek M, Yamada K, Edger PP, Miyahara M, Kondo M, Bottcher C, Mori M, Nishimura M, Schulze-Lefert P, Hara-Nishimura I, Bednarek P. PYK10 myrosinase reveals a functional coordination between endoplasmic reticulum bodies and glucosinolates in Arabidopsis thaliana. *Plant J*. 2017;89:204-20. Epub 2016/09/10.

[69] Ogasawara K, Yamada K, Christeller JT, Kondo M, Hatsugai N, Hara-Nishimura I, Nishimura M. Constitutive and inducible ER bodies of Arabidopsis thaliana accumulate distinct beta-glucosidases. *Plant Cell Physiol*. 2009;50:480-8.

[70] Nagano AJ, Maekawa A, Nakano RT, Miyahara M, Higaki T, Kutsuna N, Hasezawa S, Hara-Nishimura I. Quantitative analysis of ER body morphology in an Arabidopsis mutant. *Plant Cell Physiol*. 2009;50:2015-22.

[71] Inohara N, Nunez G. ML -- a conserved domain involved in innate immunity and lipid metabolism. *Trends Biochem Sci*. 2002;27:219-21.

- [72] Dalal J, Lewis DR, Tietz O, Brown EM, Brown CS, Palme K, Muday GK, Sederoff HW. ROSY1, a novel regulator of gravitropic response is a stigmasterol binding protein. *J Plant Physiol.* 2016;196-197:28-40.
- [73] Ichimura Y, Kirisako T, Takao T, Satomi Y, Shimonishi Y, Ishihara N, Mizushima N, Tanida I, Kominami E, Ohsumi M, Noda T, Ohsumi Y. A ubiquitin-like system mediates protein lipidation. *Nature.* 2000;408:488-92.
- [74] Harding HP, Zhang Y, Ron D. Protein translation and folding are coupled by an endoplasmic-reticulum-resident kinase. *Nature.* 1999;397:271-4.
- [75] Kleinboelting N, Hupé G, Kloetgen A, Viehöver P, Weisshaar B. GABI-Kat SimpleSearch: new features of the *Arabidopsis thaliana* T-DNA mutant database. *Nucl Acids Res.* 2012;40:D1211-5. Epub 2011/11/12.
- [76] Contento AL, Xiong Y, Bassham DC. Visualization of autophagy in *Arabidopsis* using the fluorescent dye monodansylcadaverine and a GFP-AtATG8e fusion protein. *Plant J.* 2005;42:598-608. Epub 2005/04/30.
- [77] Hajdukiewicz P, Svab Z, Maliga P. The small, versatile pPZP family of *Agrobacterium* binary vectors for plant transformation. *Plant Mol Biol.* 1994;25:989-94.
- [78] Bao Y, Wang C, Jiang C, Pan J, Zhang G, Liu H, Zhang H. The tumor necrosis factor receptor-associated factor (TRAF)-like family protein SEVEN IN ABSENTIA 2 (SINA2) promotes drought tolerance in an ABA-dependent manner in *Arabidopsis*. *New Phytol* 2014; 202: 174-187. Epub 2013/12/18.
- [79] Sheen J. A transient expression assay using *Arabidopsis* mesophyll protoplasts. 2002. http://molbio.mgh.harvard.edu/sheenweb/protocols_reg.html.

[80] Nelson BK, Cai X, Nebenfuhr A. A multicolored set of in vivo organelle markers for co-localization studies in Arabidopsis and other plants. *Plant J.* 2007;51:1126-36. Epub 2007/08/02.

[81] Robinson MD, Oshlack A. A scaling normalization method for differential expression analysis of RNA-seq data. *Genome Biol.* 2010;11:R25.

[82] Love MI, Huber W, Anders S. Moderated estimation of fold change and dispersion for RNA-seq data with DESeq2. *Genome Biol.* 2014;15:550.

ACCEPTED MANUSCRIPT

Figure Legends

Figure 1. ER stress-induced autophagy in *Arabidopsis* seedling roots is independent of *BZIP60*.

(A) Possible mechanisms by which IRE1B links ER stress to autophagy, either by *BZIP60* splicing, protein phosphorylation, IRE1B clustering or Regulated IRE1-dependent DNA Degradation (RIDDD). (B) Schematic diagram of T-DNA insertions in *bzip60* mutants. Exons and intron are depicted to scale by boxes and lines, respectively. The positions of T-DNA insertions are indicated by triangles, the numbers below show the insertion sites or start and stop codons in base pair units, and the arrows below indicate primer-binding sites. (C) RT-PCR analysis of *BZIP60* gene expression in wild-type (WT) and the 3 *bzip60* mutants using the primers depicted in (B). Total RNA was isolated from 7-day-old seedlings. AT3G18780/*ACT2* (actin 2) was used as a loading control. (D) Seven-day-old WT and 3 *bzip60* mutants were transferred to 1/2 MS liquid medium plus DMSO as control, or supplemented with 5 $\mu\text{g}/\text{mL}$ Tm for 6 h to induce ER stress. Autophagosomes were visualized by MDC staining and confocal microscopy. Bar: 50 μm . (E) The number of autophagosomes per root section was assessed following Tm treatment and staining by MDC. Error bars represent SE, $n > 20$ for 3 biological replicates. Asterisks indicate significant differences ($P < 0.05$) using the Student t test compared with WT under control conditions.

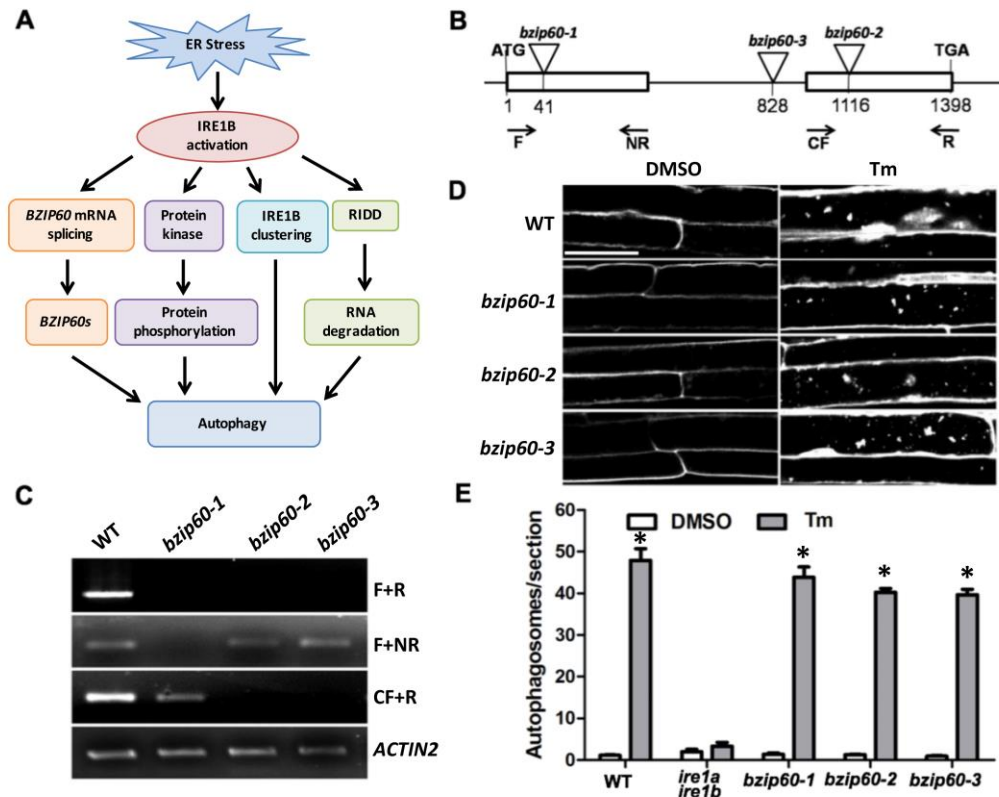


Figure 2. Complementation of autophagy defect in *ire1a ire1b* null mutant protoplasts by *IRE1B* mutant constructs. **(A)** Illustration of the disposition of IRE1B in the ER membrane. The cytoplasmic domain bears both RNase and protein kinase subdomains. Point mutations used in this study that disrupt the nucleotide binding site, kinase catalytic and RNase domains are indicated. **(B)** RT-PCR analysis of the expression of spliced *BZIP60* mRNA, *BIP3* and *IRE1B* after 6-h treatment +/- 5 μ g/mL Tm in WT and *ire1 ire1b* protoplasts, or in *ire1a ire1b* protoplasts transfected with various *IRE1B* mutants. **(C)** Protoplasts were cotransformed with GFP-ATG8E and the indicated constructs and treated as in **(B)**, and the number of successfully transformed protoplasts with active autophagy, defined as 3 or more autophagosomes per protoplast, was assessed using epifluorescence microscopy. Three replicates with 100 protoplasts per replicate were analyzed. Error bars represent SE. Asterisks indicate significant differences (*P*

< 0.05) using the Student t test compared with WT under control conditions. (D) Leaf protoplasts from WT and the *ire1a ire1b* mutant expressing GFP-ATG8E alone, or from the *ire1a ire1b* mutant background coexpressing GFP-ATG8E and *IRE1B* constructs bearing mutations as described in (A), were treated with 5 μ g/mL Tm for 6 h in the dark, then imaged by confocal microscopy. Bar: 10 μ m.

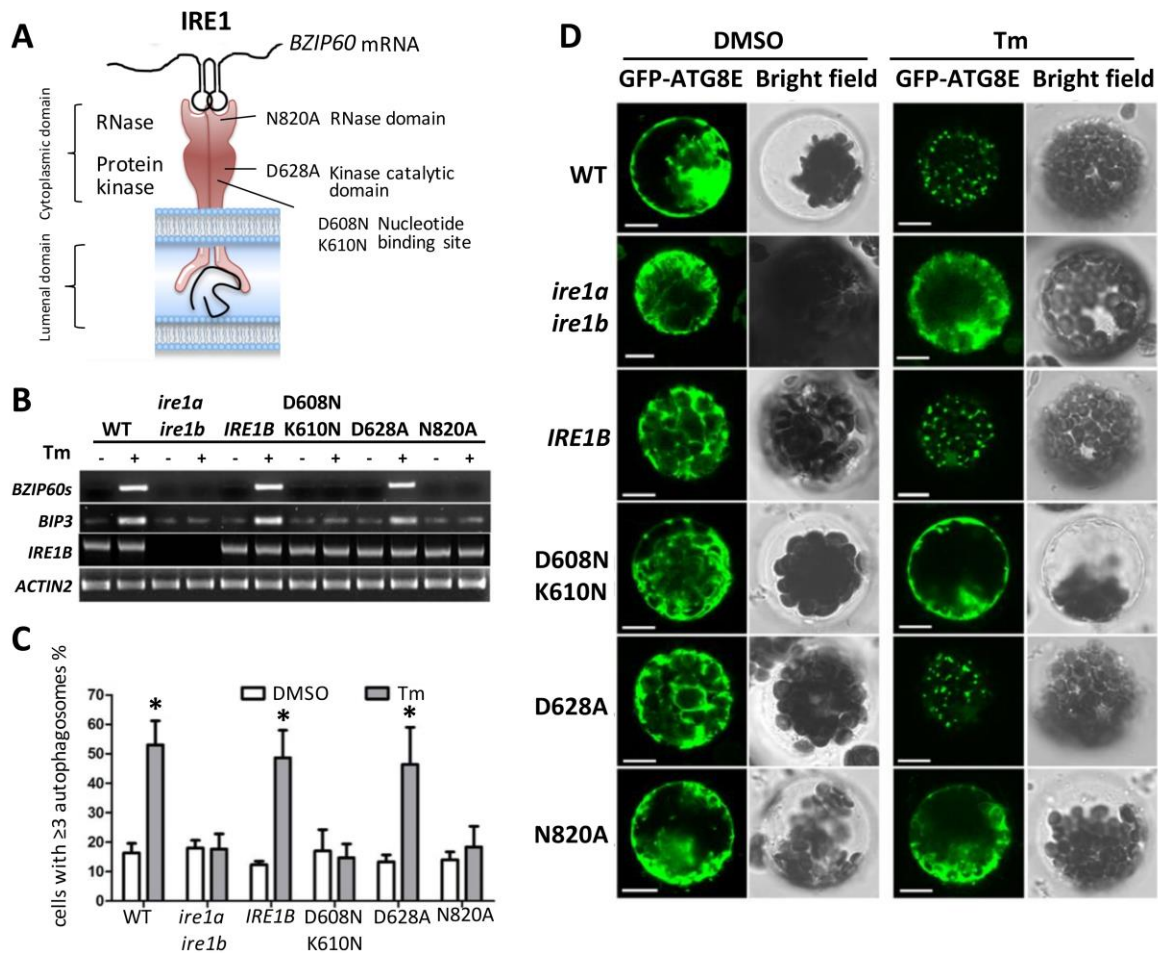


Figure 3. Complementation of defects in ER stress-induced autophagy induction in transgenic *ire1a ire1b* mutant plants bearing *IRE1B* mutant constructs. (A) Seven-day-old WT or *ire1a ire1b* seedlings expressing various *IRE1B* mutant constructs were treated in liquid 1/2 MS

medium with 5 $\mu\text{g}/\text{mL}$ Tm for 6 h and then stained with MDC. Autophagosomes were visualized by confocal microscopy, bar: 50 μm . **(B)** The number of autophagosomes in root sections was assessed by fluorescence microscopy. 15 sections per sample were analyzed, with 3 biological replicates. Error bars represent SE. Asterisks indicate significant differences ($P < 0.05$) using the Student t test compared with WT under control conditions. **(C)** Expression of *IRE1B* and *BZIP60* splicing (*BZIP60s*) in the treated seedlings was analyzed by RT-PCR. *ACT2* was employed as a loading control.

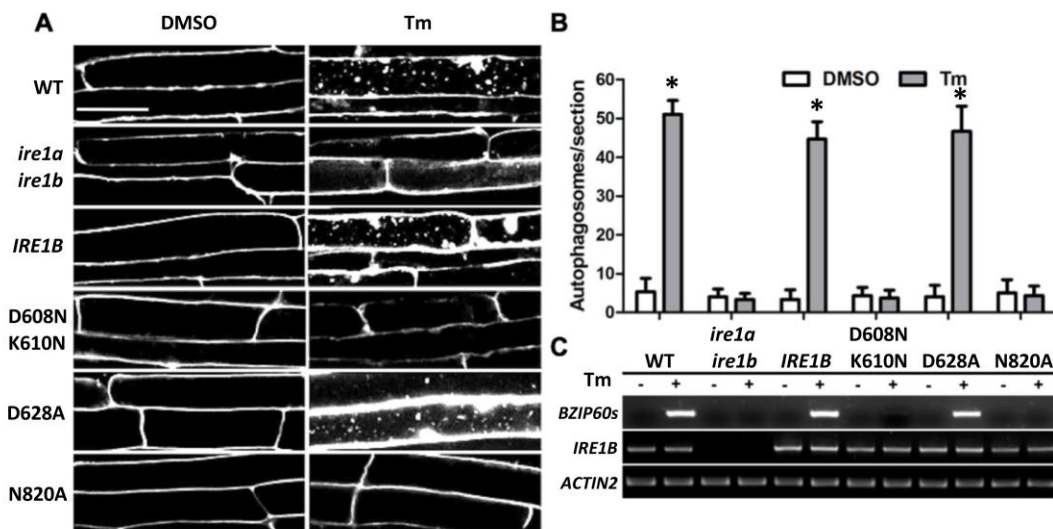


Figure 4. Clustering of IRE1B is induced upon ER stress. **(A)** *BZIP60* is spliced by IRE1B-YFP but not by the RNase dead IRE1B fusion in Tm-treated *ire1a ire1b* protoplasts. Leaf protoplasts from WT and *ire1a ire1b* plants, or protoplasts transfected with a plasmid encoding IRE1B-YFP or IRE1B^{N820A}-YFP in an *ire1a ire1b* mutant background, were incubated in the dark for 12 h, treated with DMSO (as the control) or 5 $\mu\text{g}/\text{mL}$ Tm for 6 h and RNA was extracted. RT-PCR was carried out to detect *BZIP60* mRNA splicing (*BZIP60s*), and *ACT2* was used as a loading control. **(B)** Colocalization of IRE1B with an ER marker. Protoplasts isolated from leaves of WT

plants were cotransfected with IRE1B-YFP-expressing constructs and mCherry-tagged ER or Golgi markers, incubated in the dark for 12 h and observed using confocal microscopy. Bar: 10 μm . (C) Confocal microscopy analysis of the clustering of IRE1B-YFP and RNase-dead IRE1B^{N820A}-YFP. Leaf protoplasts from WT seedlings were transfected with a plasmid expressing an ER-YFP marker, IRE1B-YFP or RNase dead IRE1B^{N820A}-YFP, incubated in the dark for 12 h, and then treated with DMSO or 5 $\mu\text{g}/\text{mL}$ Tm for 6 h before imaging by confocal microscopy. Bar: 10 μm . (D) Quantitation of the number of clusters per cell for at least 9 protoplasts/treatment derived from images such as those shown in (C), with 3 biological replicates. Error bars = SD.

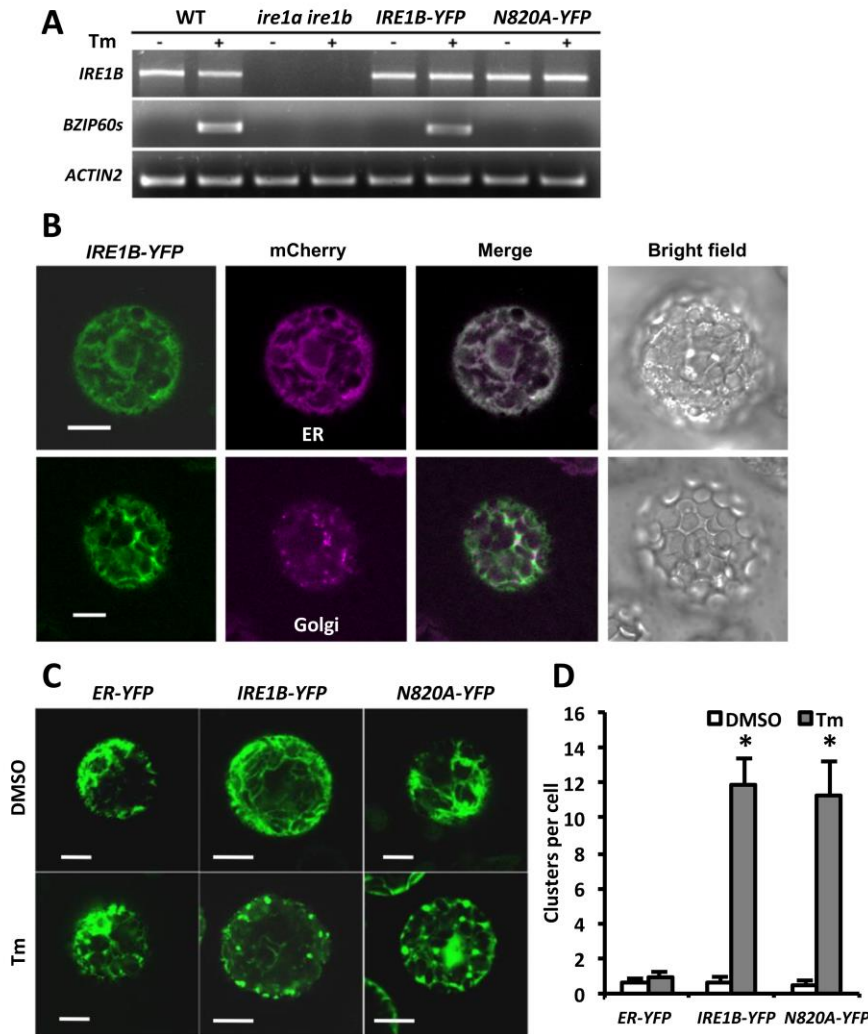


Figure 5. Some RIDD target genes repress ER stress induced autophagy. **(A)** Suppression of autophagy induction by transfecting WT leaf protoplasts with RIDD target genes. The top 12 RIDD target genes expressed from a 35S promoter were introduced into protoplasts together with GFP-ATG8E. After incubation in the dark for 12 h, samples were treated with DMSO (as the control) or 5 μ g/mL Tm for 6 h. Autophagosomes were quantified and normalized to WT protoplasts transfected with the empty vector (Control) with DMSO treatment. The average of 3 biological replicates is shown, with 100 protoplasts per replicate, and error bars represent SE. **(B)** Inhibition of RIDD target gene translation results in failure of autophagy suppression.

ROSY1/ML, *PR-14* and *BGLU21* and mutant forms of each (*mROSY1/mML*, *mPR-14* and *mBGLU21*) with a mutated start codon were expressed from a 35S promoter in protoplasts with GFP-ATG8E. Protoplasts were treated and examined as in (A). (C) Overexpression of RIDD target genes has no effect on sucrose starvation-induced autophagy. RIDD target genes were coexpressed in protoplasts with GFP-ATG8E and incubated in the presence or absence of 0.5% sucrose for 2 days in the dark. Autophagosomes were quantified and normalized to WT protoplasts transfected with the empty vector (Control). The average of 3 biological replicates is shown, with 100 protoplasts per replicate, and error bars represent SE. For all experiments, asterisks indicate significant differences ($P < 0.05$) using the Student t test compared with vector alone under control conditions.

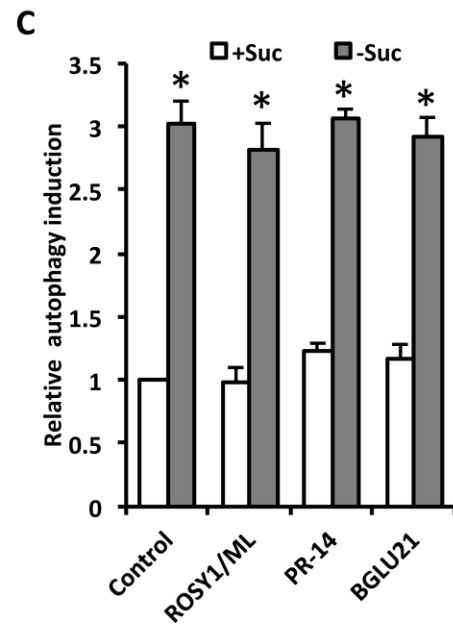
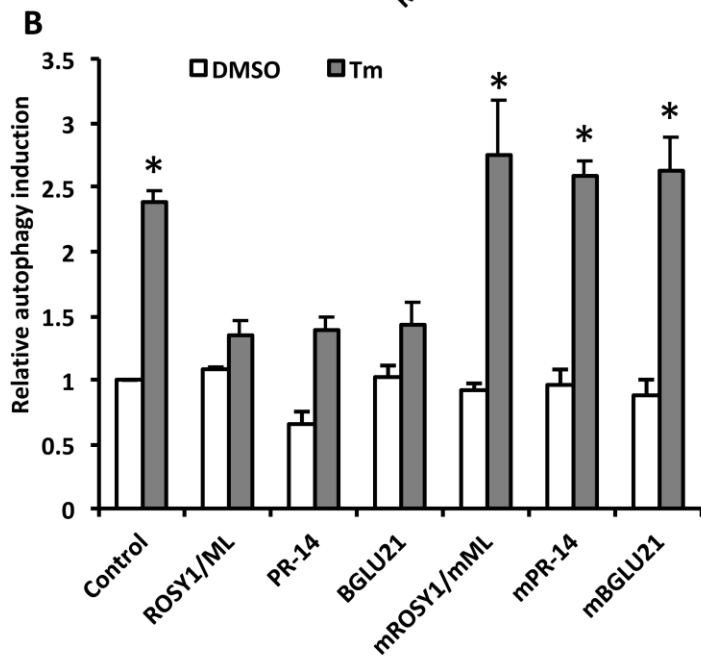
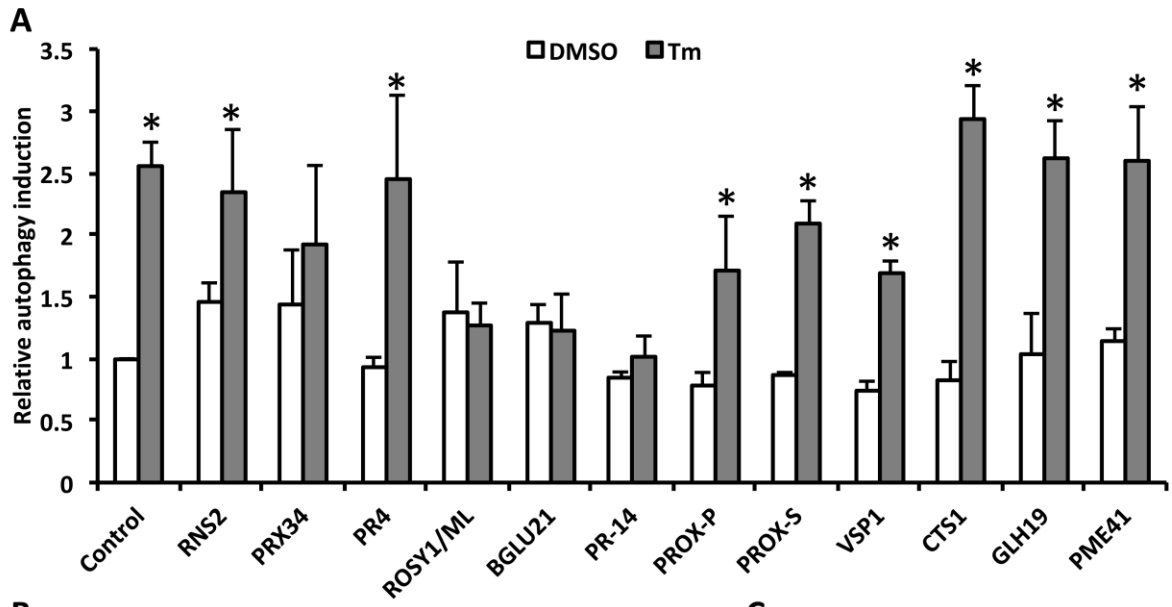


Table 1. Top 12 genes most highly spared of downregulation in *ire1a ire1b* null mutants compared to WT, and in an *ire1b* null mutant alone compared to WT.

Locus	<i>ire1a ire1b</i> *	<i>ire1b</i> **	<i>WT</i> ***	Name/Description
AT4G36430	3.52	2.81	-1.04	<i>PROX-S</i> /Peroxidase
AT2G43620	2.48	1.72	-2.41	<i>CTS1</i> /Chitinase
AT5G24780	2.30	1.92	-2.50	<i>VSP1</i> /Veg Storage protein 1
AT3G49120	2.20	0.95	-2.30	<i>PRX34</i> /Peroxidase
AT2G43610	2.09	1.10	-2.07	<i>GLH19</i> /Glycoside hydrolase 19
AT3G04720	1.97	0.77	-2.13	<i>PR4</i> /Pathogenesis related 4
AT1G66270	1.78	0.69	-2.99	<i>BGLU21</i> /β-glucosidase 21
AT2G38390	1.69	1.73	-2.41	<i>PROX-P</i> /Peroxidase
AT4G02330	1.63	0.69	-1.29	<i>PME41</i> /Pectinase
AT2G39760	1.09	0.53	-1.00	<i>RNS2</i> /Ribonuclease 2
AT5G01870	1.61	1.37	-1.35	<i>PR-14</i> /Lipid transfer protein
AT2G16005	1.21	1.94	-1.64	<i>ROSY1/ML/MD2</i> -related lipid protein

Numbers are log₂ ratio. Data were obtained from the transcriptomic data deposited in the Gene Expression Omnibus database under accession number GSE99576.

*Log₂ fold change (fc) for *ire1a ire1b* vs *WT*, both treated with Tm

**Log₂ fc for *ire1b* vs *WT*, both treated with Tm

***Log₂ fc Tm treated *WT* vs. untreated *WT*

All edits have been made as requested and the majority of changes accepted. In cases where a change has been modified, an explanation has been included in the comment box.

ACCEPTED MANUSCRIPT

Table S1. Primers used in this study.

Primers used for RT-PCR			
Gene/primer	AGI* code	Forward Primer 5' - 3'	Reverse Primer 5' - 3'
<i>bZIP60s</i>	AT1G42990	GAAGGAGACGATGATGCTGTGGCT	AGCAGGGAACCCAACAGCAG
<i>bZIP60</i>	AT1G42990	ATGGCGGAGGAATTTGGAAGC	TCACGCCGCAAGGGTTAAGA
<i>bZIP60NR</i>	AT1G42990	/	ATCCGGTGAAGACTGAAGAA
<i>bZIP60CF</i>	AT1G42990	CCCTTATATGTCCACACAAAAG	/
<i>IRE1B</i>	AT5G24360	ATGACAAATCTATCTCCAATCAAATCT	CTACTCGAGGAATACAGTGG
<i>actin 2</i>	AT3G18780	GGAAGGATCTGTACGGTAAC	GGACCTGCCTCATCATACT
Primers used for genotyping			
T-DNA primers	5' - 3'		
LBa1	TGGTTCACGTAGTGGGCCATCG		
pAC161-LB1	CAAGGCATCGATCGTGAAGTTTC		
Primers used for cloning			
Gene	AGI code	Forward Primer 5' - 3'	Reverse Primer 5' - 3'
<i>PRX34</i>	AT3G49120	CGCGGATCCATGCATTTCTCTTCGTCTTCA	CGCGTCGACTCACATAGAGCT
<i>PR4</i>	AT3G04720	CGCGGATCCATGAAGATCAGACTTAGCATAACCA	CCGCTCGAGTCAAACGCGATC
<i>ROSY1/ML</i>	AT2G16005	CGCGGATCCATGGCGATATCTCACACCC	CGCGTCGACTCACTCGGTAAC
<i>BGLU21</i>	AT1G66270	CGCGGATCCATGGCATTGCAAAAAGTTTCCT	CGCGTCGACTTAAAGCTCATC
<i>PR-14</i>	AT5G01870	CGCGGATCCATGATGAGAGTTGTGTTACCACTA	CGCGTCGACTCACTTAATGCT
<i>PROX-P</i>	AT2G38390	CGCGGATCCATGGGGTTTTTCGTCTTCATT	CGCGTCGACTCAGATAGAACT
<i>PROX-S</i>	AT4G36430	CGCGGATCCATGGCAAGACTCACGAGCTT	CGCGTCGACTCAAGAGTTAAT
<i>VSP1</i>	AT5G24780	CGCGGATCCATGAAAATCCTCTCACTTTCCT	CGCGTCGACTTAAAGAAGGTA
<i>CTS1</i>	AT2G43620	CGCGGATCCATGGCTACCCTAAGAGCAATGT	CGCGTCGACTTAGCAACTAAC
<i>GLH19</i>	AT2G43610	CGCGGATCCATGGCGACACAAAATGCGAT	CGCGTCGACTCAACATGAGAC
<i>PME41</i>	AT4G02330	CGCGGATCCATGCTATCTCTCAAACCTTCC	CCGCTCGAGTTACGAAAGTA
<i>mROSY1/mL</i>	AT2G16005	CGCGGATCCATGCGCGATATCTCACACCC	CGCGTCGACTCACTCGGTAAC
<i>mPR-14</i>	AT5G01870	CGCGGATCCATGATCGGAGAGTTGTGTTACCACTA	CGCGTCGACTCACTTAATGCT
<i>mBGLU21</i>	AT1G66270	CGCGGATCCATGCGCATTGCAAAAAGTTTCCT	CGCGTCGACTTAAAGCTCATC

*AGI, Arabidopsis Genome Initiative